6ICEGE 6th International Conference on Earthquake Geotechnical Engineering
1-4 November 2015
Christchurch. New Zealand

Model Tests on Sand Eruption from the Liquefied Ground through the Gap of Pavement

J. Kuwano[1], R. Kuwano[2]

ABSTRACT

Significant number of subsurface cavities was found in the liquefied ground after the 2011 Great East Japan earthquake. Characteristics of subsurface cavities were investigated based on the results of the radar exploration conducted in Urayasu-city, Shinkiba-area and Narashino-city around Tokyo Bay, which suffered from damage by the ground liquefaction. It was found that the cavities tended to form near the manholes and the pavement joints. Size and shape of the cavities were larger and thinner than the cavities that were observed in the non-liquefied ground. A series of model tests was conducted in order to understand the mechanism of sand eruption and underground cavity formation caused by the liquefaction. Liquefaction and sand boiling were simulated in the model test by the upward seepage flow. With the increase in the hydraulic gradient, sand grains were moved initially horizontally then vertically, which resulted in disturbance and loosening in the ground. The flow rate at the gap of the pavement to cause sand eruption increased with the increase in the grain size. The hydraulic gradient causing sand eruption was much higher than the critical hydraulic gradient in all the test cases.

Introduction

Damage of roads was widely found in Tokyo Bay area, which suffered from damage by liquefaction, after the 2011 Great East Japan Earthquake with M=9.0. Ground penetration radar exploration from a specially equipped car running at the maximum speed of 60 km/h was carried out in Urayasu City, Shinkiba area and Narashino City for the total distance of 355 km. 709 hidden subsurface cavities were found by the radar and their characteristics were investigated (Sera et al., 2013 & 2014). Locations of liquefaction subsurface cavities were found by the investigation and are shown in Figure 1.

Cavities under roads are not always caused by ground liquefaction. Cavities in ordinary conditions are caused by other factors such as breakage of sewer pipes. Subsurface cavities of this type are formed when soil particles or sub-base materials are washed away into the pipe. A cavity thus formed from a certain depth of the ground expands with time, and when the strength of the pavement is not enough, a sudden cave-in finally occurs. Table 1 compares features of ordinary cavities and liquefaction cavities found in Tokyo Bay area. It is seen that the cavity occurrence ratio in liquefied areas is 7 times larger than that in the ordinary condition. The cavity occurrence ratios in the liquefied area are 1.06 cavities/km for arterial roads, 1.30 cavities/km for sub-arterial roads, and 2.07 cavities/km for community roads. Such difference in the cavity occurrence ratios is probably due to the difference in density of buried pipes and in the pavement structures among the roads. Many of these cavities were thin, large in area occasionally more

[1]Professor, Department of Civil and Environmental Eng., Saitama University, Japan, jkuwano@mail.saitama-u.ac.jp
[2]Professor, Institute of Industrial Science, University of Tokyo, Japan, kuwano@iis.u-tokyo.ac.jp

than 10 m^2, and made by erosion at the road sub-base leaving undulation at the cavity bottom according to the borehole camera pictures as shown in Figure 2 for example. Locations where many cavities were found coincided with large-scale sand boiling, subsidence or cave-in of the road surface. The cavities were formed especially along pavement joints and around manholes, where there were gaps of pavement, and around buried sewer line structures.

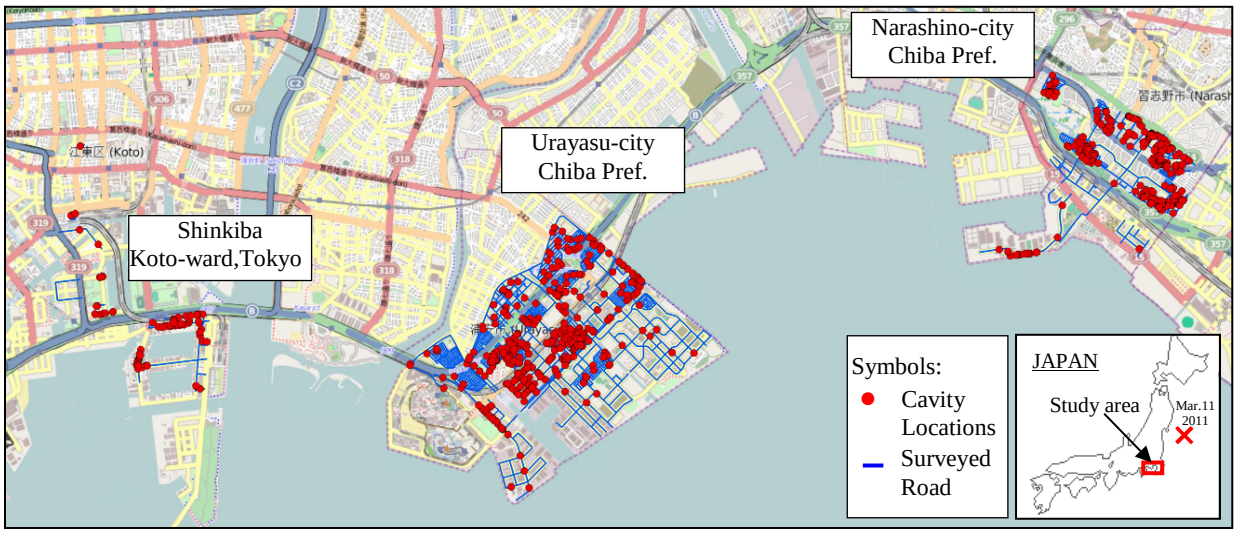

Figure 1. Locations of subsurface cavities caused by ground liquefaction.

Table 1. Summary of subsurface cavity investigation.

		Ordinary cavities	Liquefaction cavities
Occurrence ratio		0.22 cavity/km	1.56 cavity/km
Average	Area	1.68 m^2	2.38 m^2
	Thickness	0.20 m	0.13m
	Depth of cavity ceiling	0.38 m	0.37 m

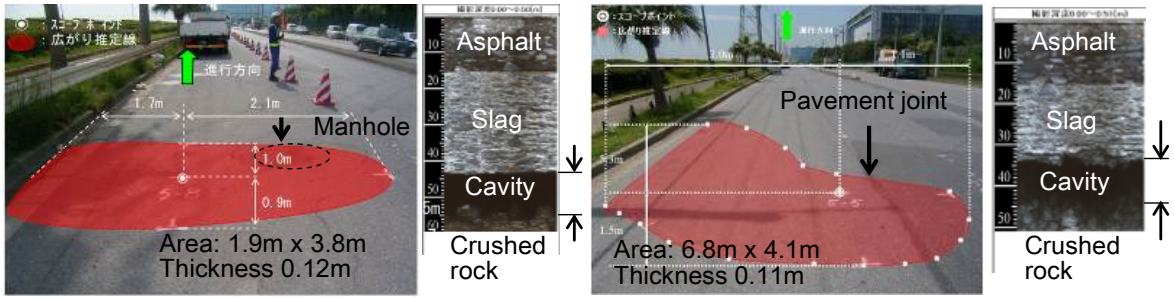

(a) Subsurface cavity around manhole (b) Subsurface cavity near pavement joint

Figure 2. Examples of liquefaction cavities.

In this study, a series of model tests was carried out in order to understand the mechanism of sand eruption from the liquefied ground through the gap of pavement and the formation of the cavity beneath the pavement. Penetration resistance was measured after the eruption test to evaluate the ground loosening that was created around the cavities.

Test Outline

A 1g prototype scale model around the gap of pavement was prepared in a soil chamber of 30cm long, 8cm wide and 20cm high, as shown in Figure 3. Water was supplied from the bottom of the model ground simulating upward seepage flow caused by liquefaction. Hydraulic gradient of the water supply could be adjusted by the elevatable water tank connected to the bottom of the soil chamber. The model ground surface was covered by an acrylic lid having a 2mm wide opening, from which boiling sand could be erupted. Water table was adjusted by draining the water from the sidewall of the chamber. Water was slowly penetrated and the model ground was saturated in advance. Then the water tank was elevated at 5 cm intervals to apply additional hydraulic gradient to generate liquefaction in the ground. Sand grains lost effective stresses and upward seepage flow caused sand eruption through the opening in the lid. After the test, water in the model ground was drained for more than 24 hours and penetration resistance was measured at five locations using a 3mm diameter needle.

In total, five tests were conducted as shown in Table 2. Silica sand No.7 was mainly used for the material of the model ground. It has mean diameter of 0.131mm. The maximum and minimum void ratios of the sand are 1.24 and 0.74 respectively. The model ground was prepared by the air-pluviation method at a relative density of approximately 75%. The permeability of the ground was around 3.83 $\times 10^{-3}$cm/s. Silica sand No.5 (D_{50}=0.360mm, k=7.17 $\times 10^{-3}$cm/s) and silica sand No.8 (D_{50}=0.0799mm, k=3.79$\times 10^{-3}$cm/s) were also used to see the effect of grain size on the sand eruption. Colored sand was put on the surface and in front of the ground, as shown in Figure 3, for the observation of sand grains' movement. In case of silica sand No.7, two additional cases were conducted, i.e. Case 1-5 in which the acrylic lid was not used to observe the effect of pavement on sand eruption, and Case 1-2 in which a model pipe with the diameter of 6 cm was buried.

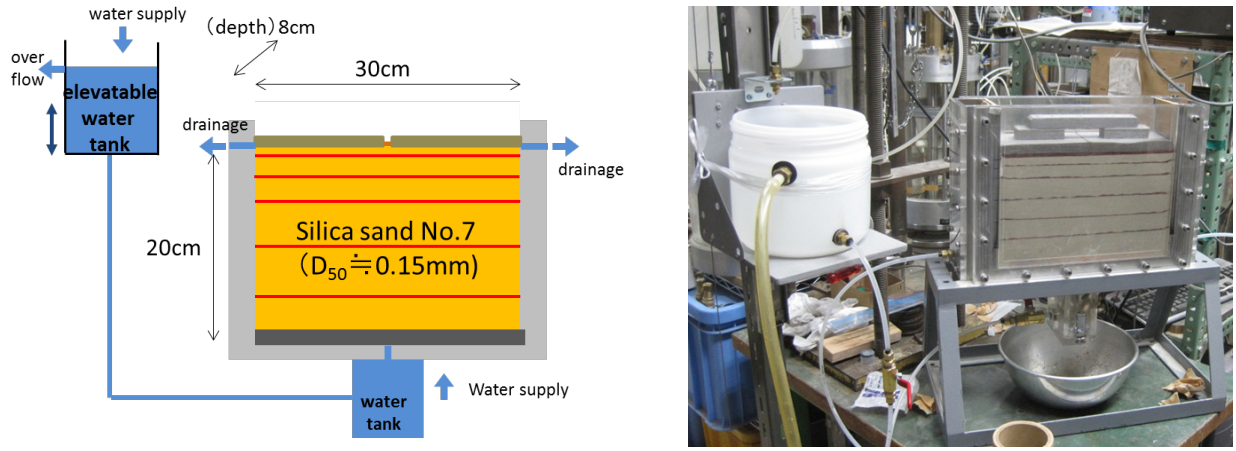

Figure 3. Schematic figure and photo of apparatus.

Table 2. Test conditions and sand eruption conditions.

Case No.	Silica sand	D_{50} (mm)	Opening at x (cm)	Pipe center (x, z)	Sand eruption condition	
					Δh (cm)	Flow rate, v (cm/s)
1-1	No. 7	0.131	0	None	25	0.660
1-2	No. 7	0.131	0	(0, -9)*	25	0.660
1-3	No. 8	0.080	0	None	15	0.539
1-4	No. 5	0.360	0	None	55	2.630
1-5	No. 7	0.131	No lid	None	60	0.011**

* The opening is at (x, z) = (0, 0). Pipe diameter is 6 cm.
** Boiling in the ground rather than sand eruption from the ground surface

Results and Discussion

In the Cases 1-1 to 1-4, in which the pavement model of acrylic lid with a 2mm wide opening at the center was set on the ground surface, with the increase in the hydraulic gradient, sand grains initially moved horizontally over the ground surface causing erosion at the ground surface and undulation at the cavity bottom as shown in Figure 4. It is similar to the subsurface cavities observed in the liquefied area. The further increase in the hydraulic gradient induced sand eruption due to the vertical movement of sand grains through the gap of the pavement model. The flow rate at which sand eruption occurred through the gap of pavement was measured by measuring the amount of drained water per unit time and is shown in Table 2.

Test conditions were the same in the Cases 1-1, 3 and 4 except the grain sizes. As seen in Table 2, the flow rate at the gap, v, that cause sand eruption increased with the increase in the grain size. Pidwirny (2006) and Yee (2012) showed the relationship between stream flow velocity and particle erosion, transport, and deposition as shown in Figure 5. Measured flow rates to cause eruption of three sands with different grain sizes are also plotted in Figure 5. It is seen that the data are located at the boundary between “Transport” and “Deposition”. Flow rate at the opening should be high enough to bring out sand grains through the gap of pavement, i.e. to cause sand eruption.

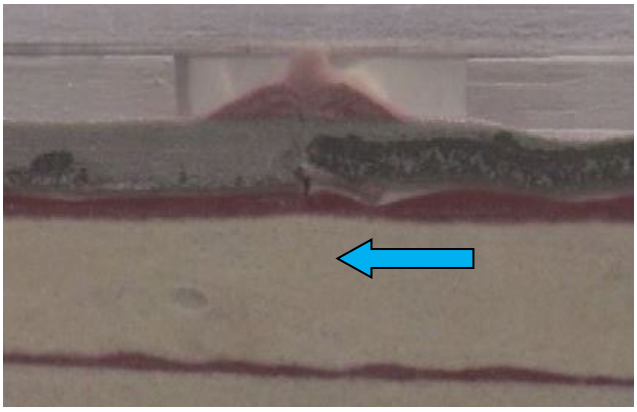

Figure 4. Horizontal movement of particles and undulated ground surface (Case 1-1, Δh=35cm).

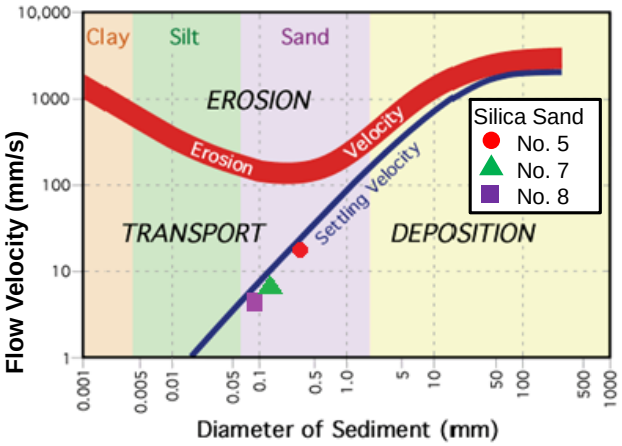

Figure 5. Relationship between grain diameter and flow velocity to start sand eruption (modified Pidwirny, 2006).

When a buried pipe was located near the opening as in the Case 1-2, water flow path seemed to concentrate initially around the buried structure, then boiling or upward turbulence flow was finally observed as shown in Figure 6. It caused serious ground disturbance and loosening as compared to the Case 1-1. However, the head difference that caused sand eruption was same, i.e. 25 cm, in both cases as seen in Table 2. The head difference of 25 cm is 1.34 times as large as 18.6 cm to cause critical hydraulic gradient in this test series.

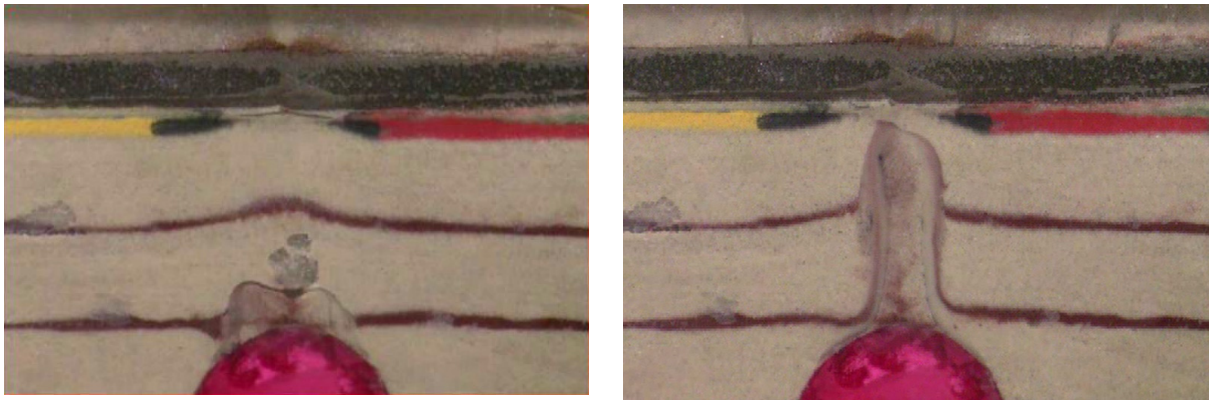

(a) Case 1-2 (Δh = 70 cm) (b) Case 1-2 (Δh = 100 cm)

Figure 6. Sand boiling above a buried pipe (Case 1-2).

When the ground surface was not covered with the pavement model in the Case 1-5, the model ground started to inflate almost uniformly at the head difference of 30 cm which is 1.61 times as large as the critical value. Thickness of the model ground increased from the original thickness of 20 cm to about 25 cm. However, further increase in the head difference of 60 cm (3.22 times as large as the critical value) resulted in the boiling or upward turbulence flow as shown in Figure 7. As the seepage flow came out almost uniformly from all the ground surface, the flow rate was as small as about 0.01 cm/s at Δh=60cm and was much lower than the value to separate

"Transport" and "Deposition" for silica sand No. 7 as shown in Figure 5. However, once the concentration of the flow started, the ground around it became looser and the flow concentration was accelerated. It resulted in boiling of the ground as shown in Figure 7. It is to be noted that in all the cases the sand ground did not show boiling at the critical hydraulic gradient, though the ground liquefied with zero effective stress.

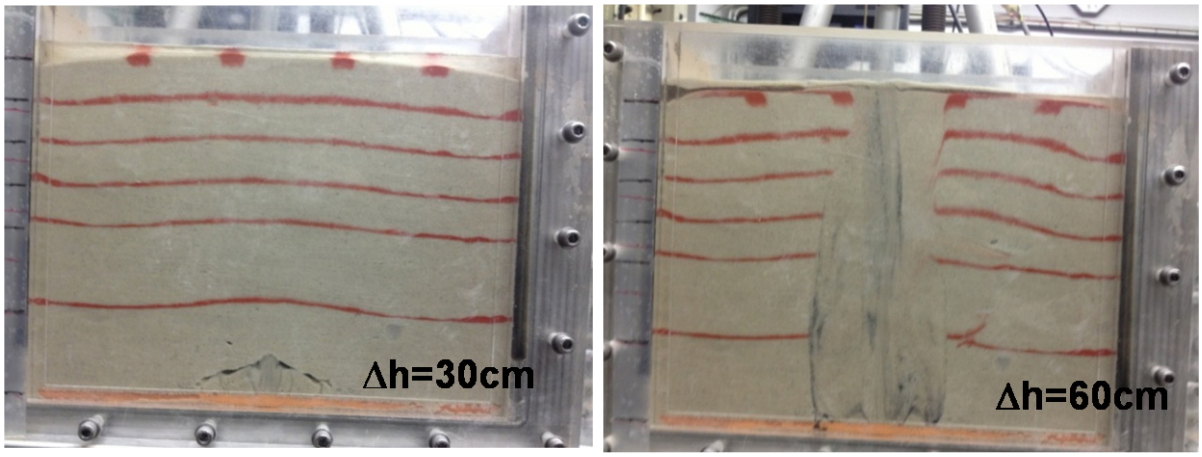

(a) Inflation of the ground (Δh = 30 cm) (b) Boiling of the ground (Δh = 60 cm)

Figure 7. Boiling of the ground without pavement (Case 1-5).

As mentioned above, the model ground was disturbed seriously by the upward seepage flow. Penetration resistance was measured at five locations using a 3mm diameter needle after the eruption test. Figure 8 shows penetration resistance at all the locations in Case 1-1'. The model condition of Case 1-1' was almost the same as that of Case 1-1 except that water was drained at z=-1.5cm and the surface layer was initially unsaturated. When the water head difference increased, inflow exceeded the drainage and the ground became almost saturated to the ground surface. Sand eruption occurred at Δh=60cm, though boiling was not observed and disturbance of the ground was thought to be much smaller than the other cases. As seen in Figure 8, penetration resistance was similar at all the locations and increased with depth, though slightly fluctuated. In contrast to Case 1-1', there was significant reduction of penetration resistance especially above and near the buried pipe in Case 1-2 as seen in Figure 9. It was due to the serious disturbance of the ground.

Conclusions

A series of model tests was conducted to simulate sand eruption and subsurface cavity in the liquefied ground. Following conclusions were drawn from the study.

The cavity occurrence ratio in liquefied areas was 7 times larger than that in the ordinary condition. Many of these cavities were thin, large in area, and made by erosion at the road sub-base leaving undulation at the cavity bottom.

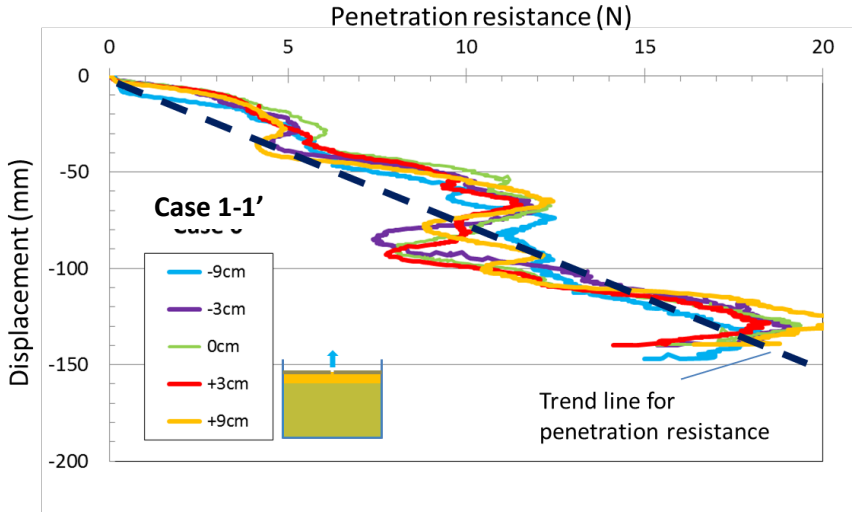

Figure 8. Penetration resistance after the test (Case 1-1')

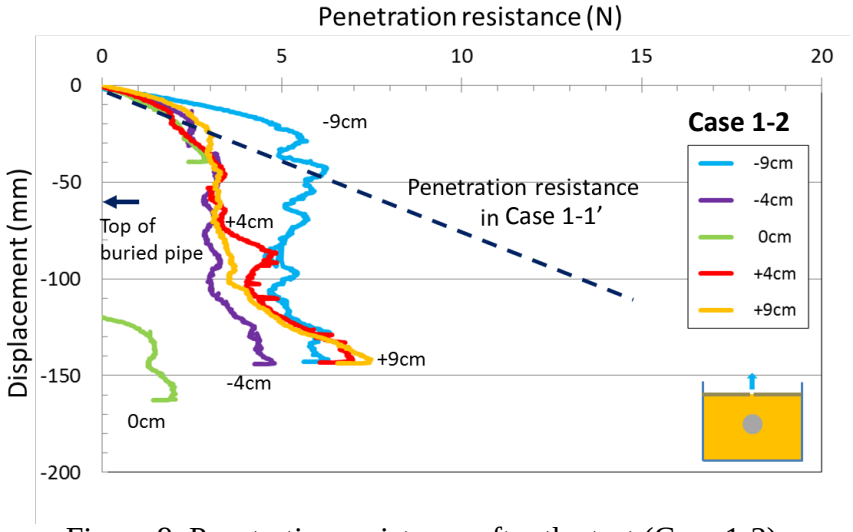

Figure 9. Penetration resistance after the test (Case 1-2)

Horizontal movement of sand grains was observed in the early stage of sand boiling. When larger hydraulic gradient was applied, vertical movement of sand occurred.

Flow rate at the opening should be high enough to bring out sand grains through the gap of pavement. The sand ground did not show boiling at the critical hydraulic gradient, though the ground liquefied with zero effective stress.

When the scale of sand boiling was large, the ground became loose especially around the buried structure because of the disturbance caused by vertical sand movement along the water flow paths.

Acknowledgments

The authors wish to thank Mr. Y. Koike and Ms. R. Sera, GEO SEARCH Co. Ltd., for providing the information of field investigation, and Mr. S. Taira and Mr. T. Hofuku, former students of Saitama University, for their effort of laboratory tests.

References

Pidwirny, M. *Erosion and Deposition. Fundamentals of Physical Geography, 2nd Edition*. Viewed on Sep 11, 2014, http://www.physicalgeography.net/fundamentals/10w.html, 2006.

Sera, R., Koike, Y., Nakamura, H., Kuwano, R. and Kuwano, *J. Survey of sub-surface cavities in the liquefied ground caused by the Great East Japan Earthquake*, *Proceedings of International Symposium on New Technologies for Urban Safety of Mega Cities in Asia (USMCA2013)*, Hanoi, Vietnam, 369-380, 2013.

Sera, R., Koike, Y., Nakamura, H., Kuwano, R. and Kuwano, *J. Sub-surface cavities in the liquefied ground caused by the Great East Japan Earthquake*, *Geotechnical Engineering Journal*, Japanese Geotechnical Society, **9**(3), 323-339, 2014 (in Japanese).

Yee, T.W. Geosynthetics for erosion control in hydraulic environment, *Proceedings of the 5th Asian Regional Conference on Geosynthetics* (Geosynthetics Asia 2012), Bangkok, Thailand, 119-134, 2012.